



ORIGINAL ARTICLE

Enrichment and recycling of Zn from electroplating wastewater as zinc phosphate via coupled coagulation and hydrothermal route



Rui Bian ^a, Ting Su ^a, Yidi Gao ^a, Yu Chen ^a, Suiyi Zhu ^{a,*}, Chenggui Liu ^a,
Xianze Wang ^{a,*}, Zhan Qu ^{a,b}, Yuxin Zhang ^a, Hong Zhang ^a

^a School of Environment, Northeast Normal University, Changchun 130117, China

^b School of Environment, Nanjing University, Nanjing 210008, China

Received 9 September 2021; accepted 19 December 2021

Available online 23 December 2021

KEYWORDS

Electroplating sludge;
Phosphate;
Hydrothermal;
Fe/Al separation;
Giniite

Abstract Electroplating is a common process of converting zinc ion in electrolyte as a micro level zinc layer on electroplating pieces. After electroplating, the remaining electrolyte on the surface of the pieces is washed with water, and accordingly, Zn-containing electroplating wastewater is generated. Hazardous Zn-containing wastewater is generated during the washing of electroplating pieces and plating tank. Herein, Zn was enriched from wastewater by commercial flocculant and then recycled as highly purified zinc phosphate via coupled acid extraction and hydrothermal treatment. Firstly, 98.4% Zn was recovered as sludge from wastewater by adding 0.2 g/L of flocculant. Then, the sludge was dissolved into an acid solution to produce a leachate with 31.2/10.8/19.3 g/L of Fe/Al/Zn and then hydrothermally treated to remove Fe/Al. The Fe removal rate was only 54.2% without phosphate and glucose but was increased to 98.6% after the addition of 0.5 g of glucose with Al/Zn loss < 2%. However, when 0.5 g of glucose and 15 g/L of phosphate were used, 99.8% Fe and 96.6% Al were synchronously removed as giniite with Zn loss < 2%. After Fe/Al separation, the remaining Zn was finally recycled as Zn phosphate particles with 98.1 wt% Zn₃(PO₄)₂·2H₂O. The added phosphate predominated the synergy removal of Fe/Al and especially lowered the Gibbs value of Al hydrolysis from 39.7 kJ/mol of boehmite to -5.96 kJ/mol of giniite, thereby reducing start-up temperature and reaction time. The proposed method showed practical application in the enrichment and recycling of valuable metals from wastewater.

© 2021 The Author(s). Published by Elsevier B.V. on behalf of King Saud University. This is an open access article under the CC BY-NC-ND license (<http://creativecommons.org/licenses/by-nc-nd/4.0/>).

* Corresponding authors.

E-mail addresses: papermanuscript@126.com (S. Zhu),
Wangxz940@nenu.edu.cn (X. Wang).

Peer review under responsibility of King Saud University.



1. Introduction

Galvanised parts are heavily used in the assembly of automobile and high-speed rail in northeast China. To produce adequate galvanised parts, Zn electroplating is widely used, where the raw parts are immersed into a Zn-containing electrolyte, and then a micro thick Zn layer is plated on parts in the electric field. After galvanisation,

the parts are washed with water to flush the remaining electrolyte on their surfaces. This process inevitably discharges Zn-containing electroplating wastewater (Bahrodin et al., 2021, Hosseini et al., 2016, Llyang et al., 2004). Whilst Zn electroplating is operated, Zn-bearing wastewater is discharged from washing the electroplating pieces. Such wastewater should be completely recycled in accordance with legal regulation (Hosseini et al., 2016). As a heavy metal with a high environmental risk, Zn removal and treated wastewater recycling are preferentially considered by many approaches, including extraction, coagulation and electrolysis (Esm et al., 2020, Rahman et al., 2021, Wahaab et al., 2013, Zhao et al., 2010). Coagulation is easily operated and widely applied in electroplating wastewater treatment, but it generates electroplating sludge at mass production (Bahrodin et al., 2021, Yu et al., 2017, Zhong et al., 2017).

Electroplating sludge is conventionally collected by a governmental company and disposed by solidification and landfill (Hosseini et al., 2016) without recycling valuable Zn (Zhong et al., 2017). Zn recycling has two merits, namely, reducing waste sludge output and obtaining new valuable product (Bian et al., 2021). Recovering Zn from electroplating sludge is an optimal route for reducing sludge production and controlling its potential pollution risk. In the sludge, Zn accounts for 0.1–48.9% (Table S1) and can be enriched/separated mainly in two categories, namely, pyrometallurgy and hydrometallurgy. Pyrometallurgy is a common route for calcinating sludge with the volatilisation of Zn powder at a high temperature. For instance, Li and Ma directly employed a vacuum reduction and distillation process to treat jarosite sludge at 1000 °C for 90 min with the addition of 29.6% coke and 13% lime powder, and obtained Zn/Pd mixture with the rest of Fe in the pyrometallurgy slag (Li and Ma 2017). Accordingly, resistance heated vacuum distillation system (Gopala et al., 2010) and/or super gravity separation method (Meng et al., 2018) were also developed to lower calcination temperature and save extra energy consumption, with the inevitable decrease of Zn recovery efficiency. Different from pyrometallurgy, hydrometallurgy consumed abundant alkaline/acid and comprised multiple steps to separate Zn at relatively low temperatures, with the inevitable formation of secondary waste liquid. Purified Zn-bearing solution was obtained after the selective leaching of spent Zn/Mn battery (Nogueira and Margarido 2015, Sadeghi et al., 2017) and zinc dross (Huajun et al., 2008) with strong alkaline and/or ammonium chloride solution in spite of the high retention of Zn in undissolved substance. Impure Al and Si were minimal in battery and dross but rich in Zn-bearing sludge. Given that Al and Si were zwitterionic, coleaching of Al/Si with Zn produced a leachate with high concentrations of Al/Si/Zn. To date, the selective separation of Zn from alkaline leachate is also a challenge due to the lack of effective extraction agent and/or precipitation route. Thus, acidic leaching is an alternative route in hydrometallurgy because it exhibits a high leaching efficiency of Zn from waste sludge and provides an optimal pH range for metal precipitation and/or extraction.

The hydrometallurgy route is effective in the resource utilisation of heavy metal-bearing smelting waste (Li et al., 2020, Rossini and Bernardes 2006) and can be considered in recycling Zn from electroplating sludge. When sludge is dissolved into a strong acid, Fe/Al impurities and Zn are released into the acid solution. Three techniques are commonly adopted for their separation (Huang et al., 2020). The first way is to extract Zn directly from the solution by adding an extractant (Pourjavid et al., 2014), e.g. tributyl phosphate (TBP) (Dessouky et al., 2008), Di-2-ethylhexyl phosphoric acid (HDEHP) (Ming et al., 2002) and dialkyldithiophosphates (Philip et al., 1986). Such extractant commonly contains the functional groups of R-POO-R', R-COO-R' and RO = P(S)S (Song et al., 2019), and shows high affinity to complex cationic Zn. However, cationic Fe/Al are active metals that can also complex with the functional groups of extractant, contaminating the expensive extractant (Samaniego et al., 2006, Weert et al., 1998). The second way is to adjust the solution pH to precipitate Fe/Al prior to Zn. However, Fe/Al hydrolysis generates Fe/Al-bearing colloid with abundant hydroxyl groups for Zn coordination (Wang and Chen 2019), leading to Zn loss in Fe/Al

precipitation. Different from the above two methods, the third way is to treat the leachate hydrothermally to accelerate Fe/Al hydrolysis at a high temperature compared with that at room temperature. Su et al., reported that 99% of Fe was precipitated as hematite from the leachate of electric arc furnace slag after treatment at 160 °C for 10 h (Su et al., 2020a,b). Liu et al., also investigated Al removal in the hydrothermal system and found that 94% Al was precipitated as boehmite particles after reaction at 270 °C for 20 h (Liu et al., 2021a,b). Such results provided new insights into Fe/Al removal prior to Zn. Process cost is an important index for Zn enrichment/recovery from wastewater. Compared with the rapid hydrolysis of cationic Fe in leachate, Al removal from leachate is performed at a high temperature for a long time, and this process is uneconomical and impractical. Thus, new methods for the effective removal of Al under relative moderate conditions are urgently demanded.

In this paper, a real electroplating wastewater was treated by commercial flocculant, and the generated sludge was recycled separately as giniite and highly purified zinc phosphate. Glucose and phosphate were added during separation to improve Fe/Al removal, and the corresponding thermodynamic analysis was performed.

2. Materials and methods

2.1. Zn-bearing wastewater pretreatment

Zn-bearing wastewater contained 81 mg/L of Zn, 1.36 mg/L of Fe, 0.62 mg/L of Al and 3.6 mg/L of nitrate at pH 4.8 whilst nitrate, phosphate and chemical oxygen demand were 3.60, 10.26 and 441.17 mg/L, respectively. It was sampled at the effluent of electroplating workplace of Jilin Sanhe Company (Changchun, China). Fig. 1 shows that 0.4 g of commercial polymeric (PAFC, Chuangshi, Zhengzhou, China) was dispersed in 2 L of wastewater to form a mixture. The mixture was stirred at 90 rpm for 10 min. During agitation, 20% NaOH solution was dropwise added into wastewater to keep the pH at 8. A brownish sludge was collected at the wastewater bottom after 2 h and then centrifugated at 5500 rpm for 5 min. Next, about 25 g of centrifugated sludge with water content of 82% was generated. A small portion of sludge was freeze-dried at – 80 °C for characterisation. The relative weight percentages of Fe, Al, Zn, Na and N were 12.6%, 5.3%, 8.7%, 2.1% and 0.03%, respectively. The crystal structure of Fe/Al/Zn-bearing deposits was analysed by X-ray powder diffraction. The surface morphology of the deposits was observed by field-emission scanning electron microscopy (Fig. 2).

The sludge was mixed with 3 M nitric acid and 2 M hydrochloric acid at the solid–liquid ratio of 0.5 under constant stirring at 90 rpm and then heated at 80 °C for 3 h. The leachate (named as Solution A) was collected and then characterised by an inductively coupled plasma optical emission spectrometer (ICP-OES, PerkinElmer, USA). Solution A contained 19.3 g/L of Zn, 31.2 g/L of Fe, 10.8 g/L of Al and 184.6 g/L of nitrate. For the prevention of potential exploding accident from nitrate decomposition in the following hydrothermal system, Solution A was then diluted by deionised water to produce Solution B.

2.2. Separation of impure Fe/Al

A hydrothermal experiment was performed to separate Fe/Al from Solution B. Firstly, 20 mL of Solution B, 0.5 g of glucose and 0.16 g of disodium phosphate were mixed in a 50 mL

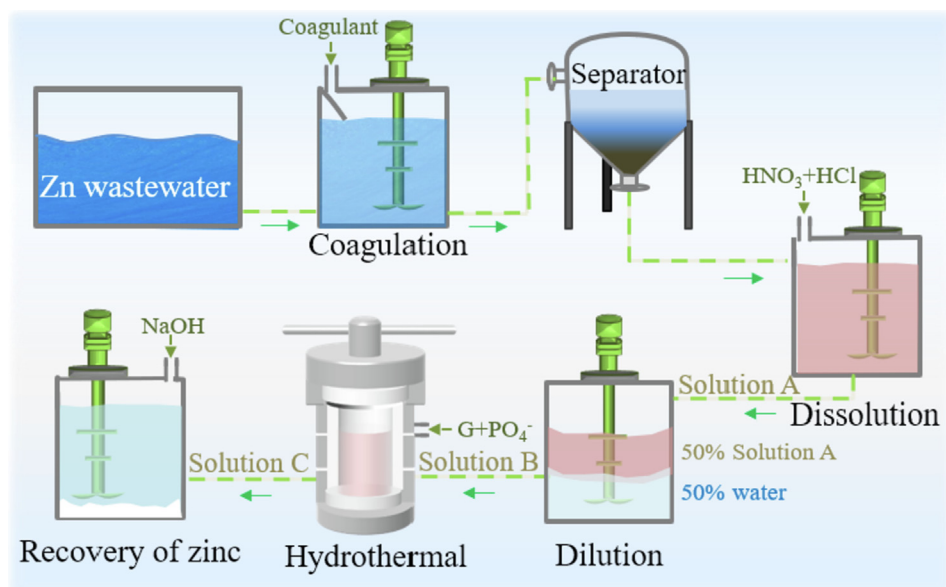


Fig. 1 Flowchart of Zn recovery from wastewater.

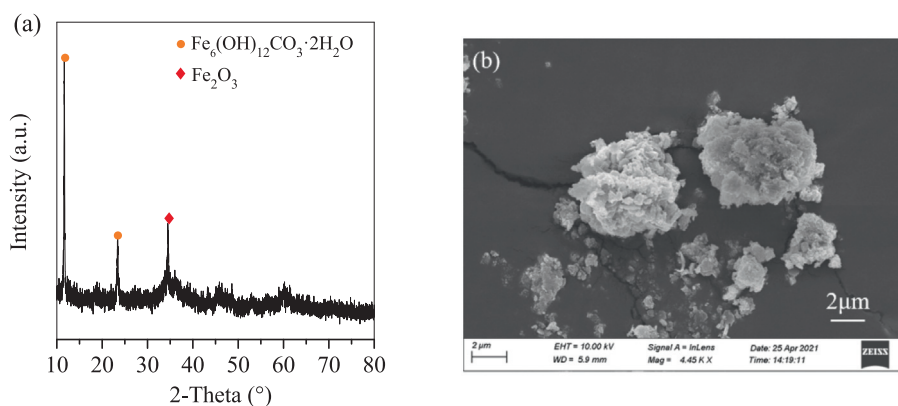


Fig. 2 (a) XRD patterns of Fe/Al/Zn-bearing deposits (b) SEM images of Fe/Al/Zn-bearing deposits.

Teflon vessel and then agitated at 125 rpm for 20 min. Then, the Teflon vessel was sealed and heated to 190 °C for 10 h. An Fe/Al-bearing precipitate was generated at the vessel bottom and then collected, and the supernatant (Solution C) was kept for Zn recovery. Fe/Al separation was optimised by varying the dosage of disodium phosphate from 0.16 g to 0.98 g, the heating temperature in the range of 130–190 °C and the reaction time of 2–20 h. A control experiment was also conducted in the absence of disodium phosphate and/or glucose according to the preceding steps.

2.3. Further precipitation of Zn in solution C

In Solution C, the Zn, Fe and Al concentrations were 9.5, 0.03 and 0.18 g/L, respectively. When the solution was adjusted to pH 5 with the addition of 4 g/L of phosphate, a new whitish precipitate was generated and collected. The collected precipitation was washed thrice with deionised water and dried at 80 °C for 5 h.

2.4. Characterisation

Total organic carbon (TOC) and pH of Solutions A/B/C were determined by a pH metre (S210-S, Mettler Toledo, US) and a TOC analyser (TOC 500; Shimadzu, Japan), respectively. Phosphate and nitrate concentrations were detected by an ion chromatograph (IC, Metrohm AG, Switzerland). Solid products were characterised by an X-ray diffractometer (XRD; Rigaku, Japan) and a scanning electron microscope (SEM; FEI Co., USA). The recovered Zn product was also analysed using X-ray fluorescence (Rint 2200, Rigaku, Japan).

3. Results and discussion

3.1. Enrichment of Zn from wastewater

The Zn-bearing wastewater was effectively treated by commercial PAFC. The Zn removal efficiency steadily increased from 34% to 98.4% with the increase in PAFC dosage from

0.05 g/L to 0.2 g/L (Fig. 3a). After treatment, a Zn-bearing sludge was generated, and the remaining wastewater contained 1.3 mg/L Zn, which met the discharge standard of electroplating industry of China (China, 2008, Daocheng and Lihui 2009). The sludge had water content of 60% and was directly leached with a mixed nitric acid and hydrochloric acid to produce Solution B with Fe, Al, Zn and nitrate concentrations of 15.6, 5.4, 9.7 and 82.3 g/L, respectively, after dilution.

For Zn recovery, Fe/Al impurities were preferentially removed via a one-step hydrothermal route. Without glucose and phosphate, only Fe precipitation was observed (Fig. 3b). The removal efficiencies of Fe/Al were approximately 0 at 130 °C but were elevated to 46.3% and 0.9%, respectively, at 160 °C and further to 54.2% and 1%, respectively, at 190 °C. This increase was accompanied by the loss of 2.4% Zn in the temperature range of 130–190 °C. This finding showed that the separation of Fe/Al impurities from Solution C was unsuccessful. When the temperature was increased from 130 °C to 190 °C, the solution pH dropped from 0.25 to 0.11,

and the nitrate concentration slightly decreased from 82.3 g/L to 69.7 g/L (Fig. 3c). With Fe removal, irregular hematite block was generated (Figs. 3d and 4). Fe removal was predominated by Fe hydrolysis at high temperature and accompanied by the release of H^+ into the solution. The thermal decomposition of nitrate occurred with temperature increase, thereby reducing its concentration (Amano et al., 2015). The removal mechanism of Fe is detailed in Section 3.4.

3.1.1. Effect of glucose on Fe/Al separation

Fe precipitation continued when glucose was added to the reaction system (Fig. 5a). When 0.5 g of glucose was added, the removal efficiency of Fe was 88.3% at 130 °C, then increased to 97.9% at 160 °C and further to 98.6% at 190 °C. These values were higher than those without glucose (Fig. 3 b). The Al/Zn removal rates were only 1.3% and 1.7%, indicating that most of Al/Zn were kept in Solution C. Nitrate concentration decreased from 82.3 g/L to 29.6 g/L with the variation of temperature from 130 °C to 190 °C,

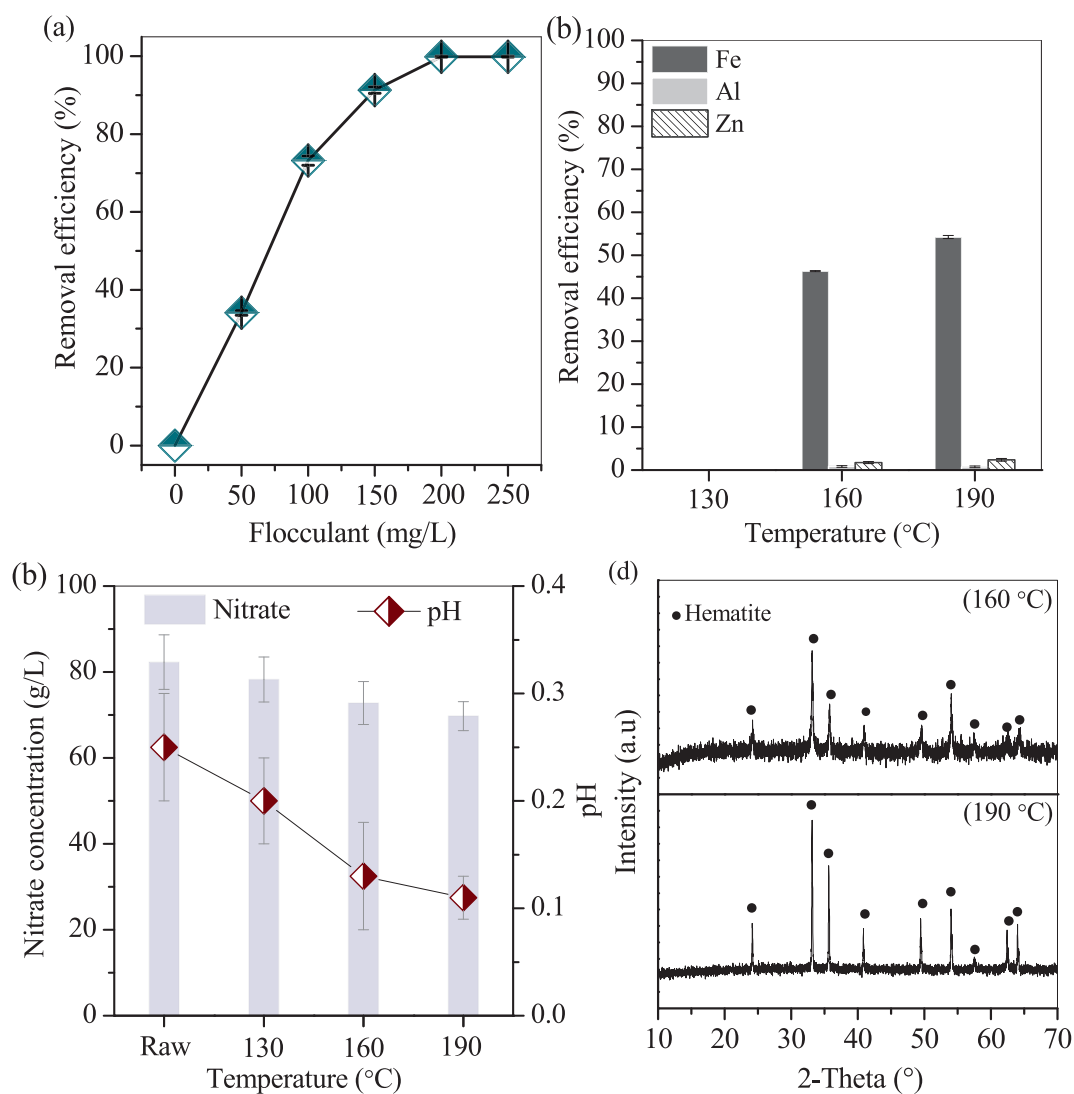


Fig. 3 Removal efficiencies of (a) Zn from wastewater and (b) Fe/Al/Zn from acid leachate without glucose and phosphate, (c) Variation of solution pH and nitration concentration and (d) XRD pattern of Fe-bearing deposits.

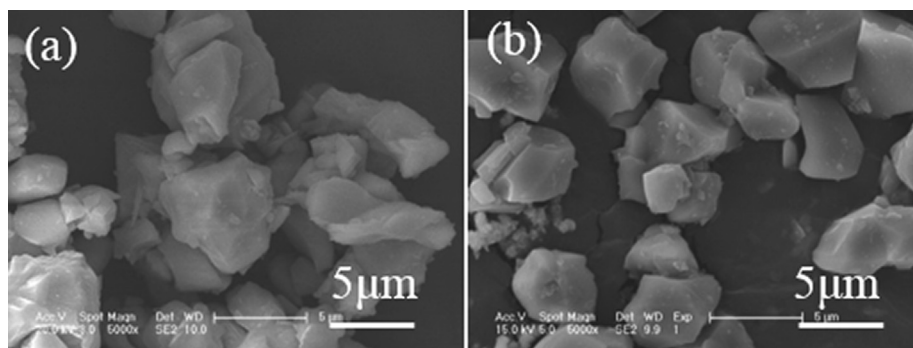


Fig. 4 SEM images of deposits generated at (a) 160 °C and (b) 190 °C without glucose and phosphate.

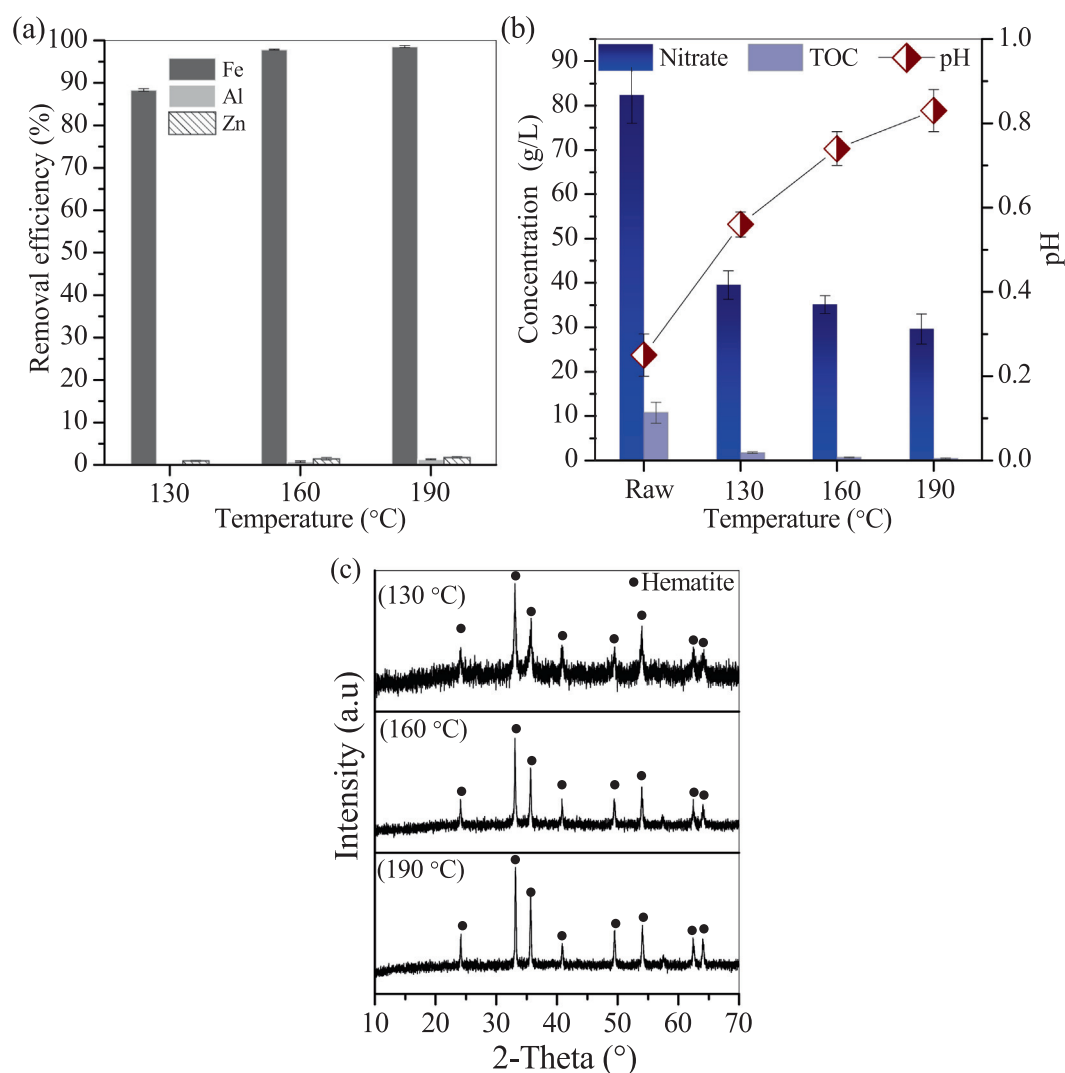


Fig. 5 (a) Removal efficiencies of Fe/Al/Zn with glucose; (b) Variation of solution pH, TOC and nitrate concentration and (c) XRD patterns of Fe-bearing deposits.

and this phenomenon was in accordance with the decrease in TOC from 10.8 g/L to 1.8 g/L at 130 °C, 0.7 g/L at 160 °C and 0.5 g/L at 190 °C (Fig. 5b). This finding was affiliated to the redox reaction of nitrate to glucose in the hydrothermal system, where H^+ was consumed and solution pH increased

from 0.25 to 0.82 (Fig. 5b) The removed Fe was involved in the hematite precipitates (Fig. 5c), which appeared as spherical particles with the diameter of 1 μ m at 130 °C (Fig. 6a) and shrunk to a diameter of 0.5 μ m at 160 °C (Fig. 6b) but were polymerised as block with coarse surface at 190 °C (Fig. 6c).

Even when the solution pH was elevated to 0.82, Al/Zn remained in the solution and were not hydrolysed in the temperature range of 130–190 °C. Such discussion is shown in Section 3.4.

3.2. Synergistic removal of Fe/Al

3.2.1. Effect of phosphate dosage on Fe/Al separation

The temperature of 190 °C was used for the synergistic removal of Fe/Al because it was optimal for Fe removal, as shown in Fig. 7. The removal efficiency of Al was only 1.4% with 5 g/L of phosphate but was increased to 49.3% with 10 g/L of phosphate, further to 96% with 15 g/L of phosphate and steadily to 97.5% with 30 g/L of phosphate. Fe removal also reached 98.7–100% in the phosphate dosage range of 5–30 g/L. However, Zn loss was lower than 2.3% in the phosphate dosage of 5–15 g/L but considerably varied to 23.8% with 30 g/L of phosphate, implying that 30 g/L of phosphate was an overdose (Fig. 7a). The solution pH was 0.82 without phosphate (Fig. 5b) but decreased to 0.5 after 5 g/L phosphate addition and slightly up to 1.28 with the phosphate dosage increased to 30 g/L. After reaction, the concentrations of the remaining nitrate and TOC were 29.6 and 0.46 g/L, respectively, without phosphate but increased to 44.3 and 2.73 g/L, respectively, after 5 g/L phosphate addition. This finding suggested that phosphate inhibited the redox reaction of nitrate to glucose. However, the concentrations of nitrate and TOC slightly decreased to 34 and 0.87 g/L, respectively, with the increase in phosphate dosage to 30 g/L (Fig. 7b and c), indicating a reverse effect to the redox reaction with low dosage of phosphate. Such performance was related to the Fe-bearing minerals, e.g. hematite and phosphate ferric. Generally, free Fe and hematite can be reduced by glucose in the hydrothermal system and then oxidised rapidly by nitrate, thus exhibiting a high catalytic effect to accelerate the redox reaction of nitrate and glucose (Qu et al., 2019). With phosphate addition, free Fe was precipitated as solid phosphate ferric by phosphate and did not participate in the redox reaction, thus leading to the retention of nitrate and glucose in the solution. However, phosphate addition also introduced H^+ into the solution, which was beneficial for the redox reaction to consume nitrate and TOC gradually. This promoting effort of H^+ was lower than that of Fe catalysis.

After the reaction, phosphate also remained in the solution, and its concentration increased from 0.4 g/L to 4.4 g/L with the addition of 5–30 g/L phosphate, suggesting that the majority of phosphate was involved in the removal of Fe/Al/Zn. The removed Fe/Al/Zn was converted into spheric particles, where

its diameter grew steadily from 2 μm with 5 g/L of phosphate (Fig. 8) to 10 μm with 15 g/L of phosphate and remained almost unchanged with 30 g/L of phosphate. This trend was consistent with the Fe/Al removal efficiencies. Corresponding EDS images showed signals of Fe/P in the four precipitates; however, the Al signal was weak with 5 g/L of phosphate, became visible with 10 g/L of phosphate and further distinct with 15 and 30 g/L of phosphate. Additionally, the Zn signal was blurry with the phosphate dosage of 5–15 g/L but became visible at 30 g/L. This trend agreed with the heavy loss of Zn (Fig. 7a). Several weak signals that belonged to the background value in the detection room of the SEM instrument were also observed (Fig. 8a and b) (Newbury et al., 2009). Al and Zn were heavily removed, but their compounds were not found in the corresponding XRD patterns. Only giniite peaks were observed. This finding revealed that the removed Al/Zn was involved in the giniite formation and accordingly, promoted the growth of giniite sphere.

3.2.2. Effect of reaction time on Fe/Al separation

The reaction time on Al removal was optimised, as shown in Fig. 9. The removal efficiency of Fe reached 99.7% in the first 2 h and remained stable in the following time. Compared with that of Fe, the Al removal efficiency was only 57.9% at 2 h but increased to 96% at 6 h and remained nearly unchanged in the time range of 6–20 h (Fig. 9a). This finding showed that Fe was removed prior to Al, and the Al removal was equilibrated at 6 h. During hydrothermal treatment, Zn loss was steadily below 3.4%, suggesting that Zn remained in the solution. Thus, the optimal reaction time was 6 h, which was lower than the 20 h for Al removal in the report of Liu et al.

After the reaction, the phosphate concentration was 2.8 g/L at 2 h and reduced to 1.07 g/L at 6 h and slowly to 1.04 g/L in the following reaction time (Fig. 9c); this trend was similar to the variation of nitrate and TOC. Conversely, the solution pH was 0.6 at 2 h but slightly increased to 0.71 at 20 h from the continuous consumption of nitrate and glucose. With Fe/Al removal, giniite spheres with average size of 2–5 μm were generated in the first 2 h but did not further grow the following time course (Figs. 9d and 10).

3.3. Precipitation of Zn from rest solution

After Fe/Al removal, over 98% Zn was kept in the solution, which was in accordance with the remaining 9.5 g/L Zn. However, the remaining Fe and Al were only 0.03 and 0.18 g/L, respectively. Such solution was adjusted to pH 5, where the remaining Zn was removed as white zinc phosphate hydrate

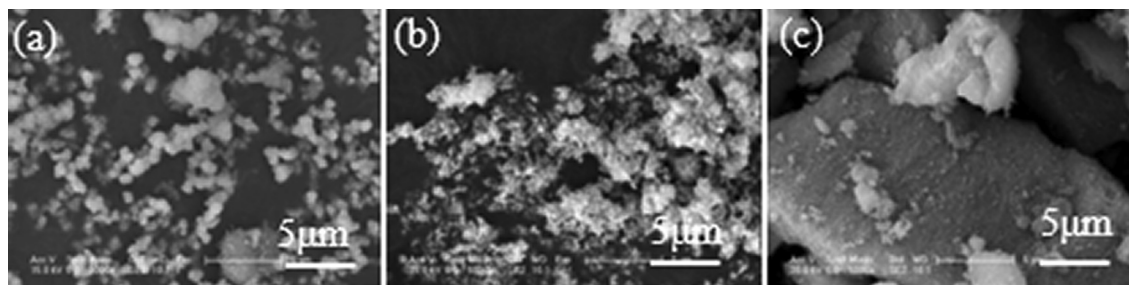


Fig. 6 SEM images of the deposits generated at (a) 130 °C, (b) 160 °C and (c) 190 °C with glucose.

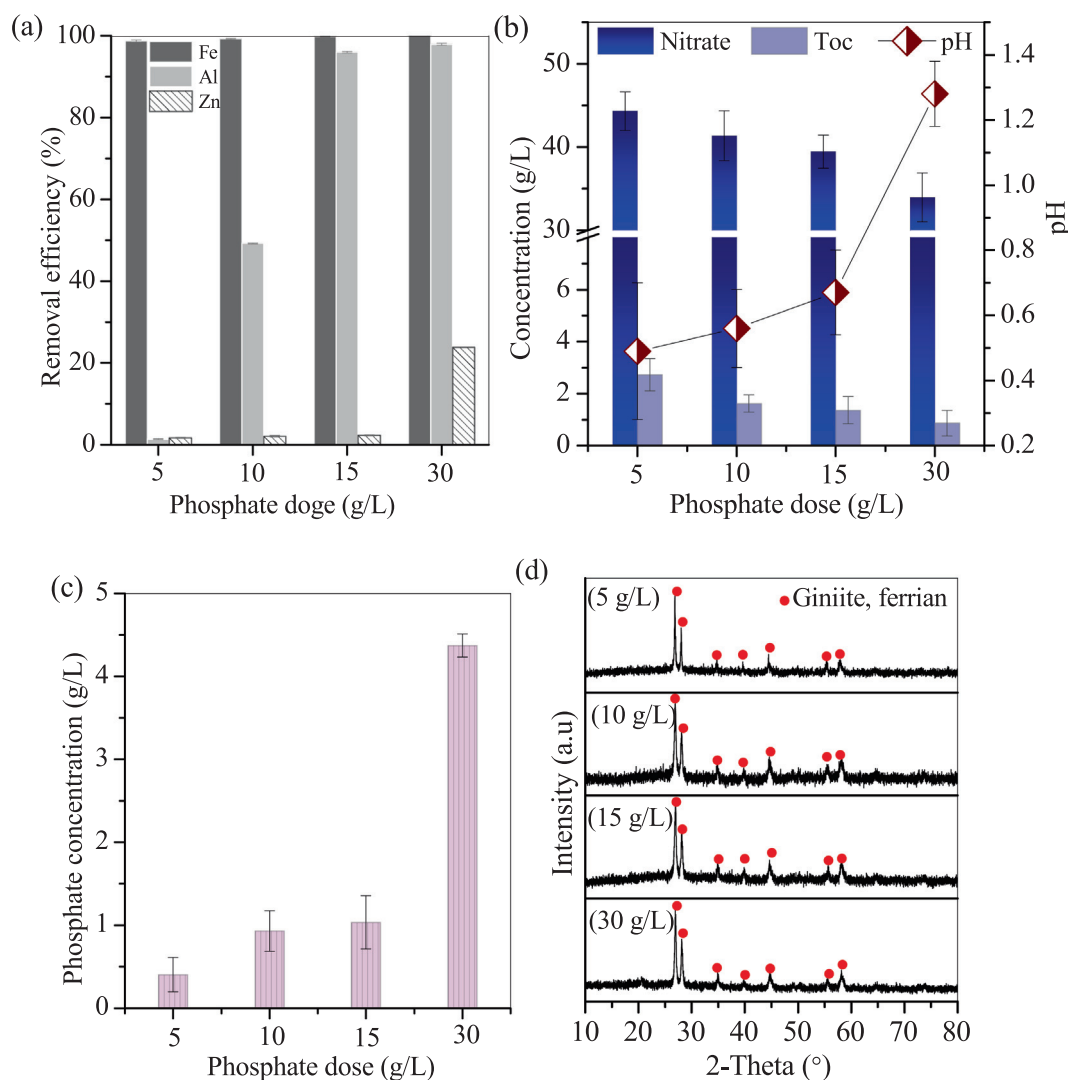


Fig. 7 (a) Removal efficiencies of Fe/Al/Zn; (b) Variation of solution pH, TOC, remaining nitrate and (c) Remaining phosphate concentrations and (d) XRD patterns of deposits.

aggregates (Fig. 11 a and b) with 98.1 wt% $\text{Zn}_3(\text{PO}_4)_2 \cdot 2\text{H}_2\text{O}$, and minor impurities of 0.12% Fe and 1.2% Al (Fig. 11c). This result showed that the recycled Zn-bearing product was highly purified.

This method left Fe/Al concentrations of only 11 and 31 mg/L, which were lower than the concentrations of residual Al left after the use of precipitant, extractant, pH adjustment and conventional hydrothermal methods. For instance, the amounts of Al and Fe removed were 10% and 89% at pH 3, respectively, and then 96.6% and 99% at pH 4.1, respectively, but approximately 29.1% of Zn precipitates at the same time because of the coprecipitation. This result indicated that pH adjustment was not effective in Fe/Al/Zn separation (Park et al., 2014). In addition, Wang et al., reported that 8.2% rare earth elements (REEs), 94.4% Al and 96.9% Fe were precipitated from REE-containing solution with 8-hydroxyquinoline overdose, and 136 mg/L Al remained (Yw et al., 2019). Fe/Al should be further removed before rare earth extraction. Compared with such methods, hydrothermal treatment was commonly used in the synthesis of nanoscale boehmite with the addition of organics. Such organics were used as a dispersing

agent to trap hydrated alumina nanoparticles and inhibit the polymerisation of the alumina nanoparticles. However, the Al removal efficiency from the reaction solution was not considered in these studies. Zhan Qu et al., precipitated 99.6% Fe in the leaching solution of electroplating waste sludge as hematite at 160 °C, but Al remained in the supernatant (Qu et al., 2021). Chenggui Liu et al., realised the coprecipitation of Fe and Al from the leaching solution of wastewater coagulation sludge, but the precipitation temperature was as high as 270 °C. Rui Bian et al., hydrothermally precipitated 98% Al from the acid solution, but the reaction temperature reached 240 °C (Bian et al., 2021). These research methods can only precipitate Fe alone under low-temperature conditions. The Fe/Al synergistic removal reaction temperature was much higher than this research and consumed more energy.

3.4. Separation mechanism of Fe/Al in the presence of phosphate

When the electroplating sludge was leached by strong acid, Fe, Al and Zn were dissolved and released into the leachate. Such heavy metals were easily hydrolysed with the increase in

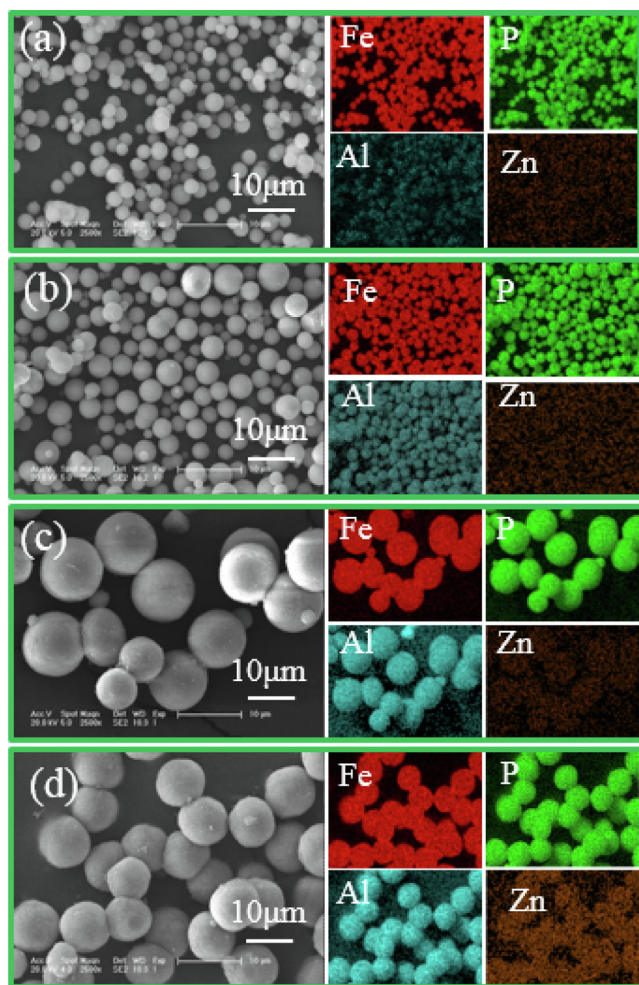


Fig. 8 SEM images and EDS patterns of deposits generated by adding (a) 5, (b) 10, (c) 15 and (d) 30 g/L of phosphate.

leachate pH. Hence, the related hydrolysis performance was analysed by using Medusa software (1.0, Royal Swedish Institute of Technology, Swiss). When the leachate was adjusted to pH 4, the hydrolysis of Fe/Al as $\text{Fe}(\text{OH})_3$ and $\text{Al}(\text{OH})_3$ was completed, but free Zn remained in the leachate (Fig. 12a). For confirmation, a precipitation experiment was conducted. The results showed that when the leachate was adjusted to pH 4, the Zn loss approached 20.3%, along with the removal of 99.8% Fe and 90.6% Al. These findings differed from those provided by the Medusa software because Fe/Al removal produces $\text{Fe}(\text{OH})_3$ and/or $\text{Al}(\text{OH})_3$ -bearing colloid with many hydroxyl groups for Zn coordination. Thus, the effective separation of Fe/Al without Zn loss from Zn-bearing solution cannot be achieved by pH adjustment.

High temperature is an alternative condition to accelerate Fe/Al removal. When the temperature increased from 25 °C to 50 °C and 190 °C, the Gibbs value of Fe hydrolysis decreased from 4.5 kJ/mol to below zero and further to -67.2 kJ/mol. This finding revealed that free Fe was stable at room temperature but started to hydrolyse at 50 °C and accelerated at 190 °C. With continued Fe hydrolysis, H^+ was released and accumulated in the solution, thus decreasing the solution pH and inhibiting Fe hydrolysis (Eq. (1)). Thus, a

portion of Fe remained in the solution. H^+ was generated from Fe hydrolysis but can be consumed in the redox reaction of nitrate to glucose (Eq. (2)). Thus, Fe hydrolysis continued, resulting in Fe remaining in the solution at a low level. Additionally, Fe was hydrolysed as Fe oxyhydroxide colloid and then aggregated in the block form without glucose (Su et al., 2020a,b). The added glucose attached to the surface of Fe oxyhydroxide colloid via electrostatic incorporation to retard the colloid aggregation and generate fine particles. In the hydrothermal system, Fe-bearing oxyhydroxide was also converted to hematite via the conjunction reaction between adjacent Fe-OH groups with the release of water molecules (Zhu et al., 2020). Such conversion did not change the morphology of Fe-bearing precipitates. Given that only nitric and hydrochloric acids were used for the sludge dissolution, nitrate and chloridion were only introduced but did not participate in Fe precipitation. Although the Fe-bearing colloid and hematite particles consisted of many hydroxyl groups, the H^+ on the hydroxyl groups did not dissociate in strong acid solution and were not replaced by cationic Al/Zn. Hence, Al/Zn almost remained in the supernatant. Different from Fe, Al and Zn were stable in the acid solution and did not hydrolyse in the condition. This finding was consistent with the positive Gibbs value of Al/Zn hydrolysis at the temperature of 20–190 °C (Fig. 12b).

With phosphate addition, the synergetic removal of Fe/Al transpired, and two new precipitation reactions of Fe/Al occurred via Eqs. (3)–(5). Such reactions were also analysed by HSC Chemistry software (9.5, Metso Outotec, Finland), as shown in Fig. 12(c). Fe was rapidly hydrolysed with phosphate, alongside Al removal. This effect differed from that in the absence of phosphate. For instance, Al hydrolysis did not occur in the reaction without phosphate, and positive Gibbs values were observed in the range of 25–190 °C (Fig. 12b). After phosphate addition, the Gibbs value of Al/phosphate reaction was reduced to below zero at 150 °C and further dropped to -16.9 kJ/mol at 190 °C. This finding suggested that the reaction of Al to phosphate occurred at 150 °C and accelerated at 190 °C. Thus, 96% Al removal was achieved with the addition of phosphate. Although more than 99% and 96% Fe/Al were removed, only giniite sphere was formed, and no Al-bearing mineral was recorded. Hence, the removed Al might be involved in Fe precipitation. The giniite product has a special formula of $\text{Fe}_5(\text{PO}_4)_4(\text{OH})_3 \cdot 2\text{H}_2\text{O}$, in which Fe^{3+} is embedded in the space structure of phosphonate-based hybrid bond and is easily replaced by free Al^{3+} to form a stable Fe/Al-bearing spheric structure (Martins et al., 2021, Rueff et al., 2016). The byproducts of $\text{Al}(\text{PO}_4)_4(\text{OH})_3 \cdot 2\text{H}_2\text{O}$ and $\text{Fe}_5(\text{PO}_4)_4(\text{OH})_3 \cdot 2\text{H}_2\text{O}$ were also reported as antirust coating and cathode material (Han et al., 2016, Mandal et al., 2010), and accordingly, had potential application in an industrial scale. Such byproducts were fine micro spheres and showed ideal functional groups to coordinate noble metal and/or enzyme, and/or to be served as a catalyst for contaminant removal (Kim et al., 2007, Muneyama et al., 1996). The byproducts exhibited good performance in the removal of Cr, Cu and Ni, similar to β -ketoenamine linkage, Fe_3O_4 -modified biochar and common adsorbents of activated carbon and molecular sieve (Han et al., 2016, Wang et al., 2020, Yang et al., 2019, Zhong et al., 2020) (Dai et al., 2019, Fl et al., 2021, Liu et al., 2021a,b).

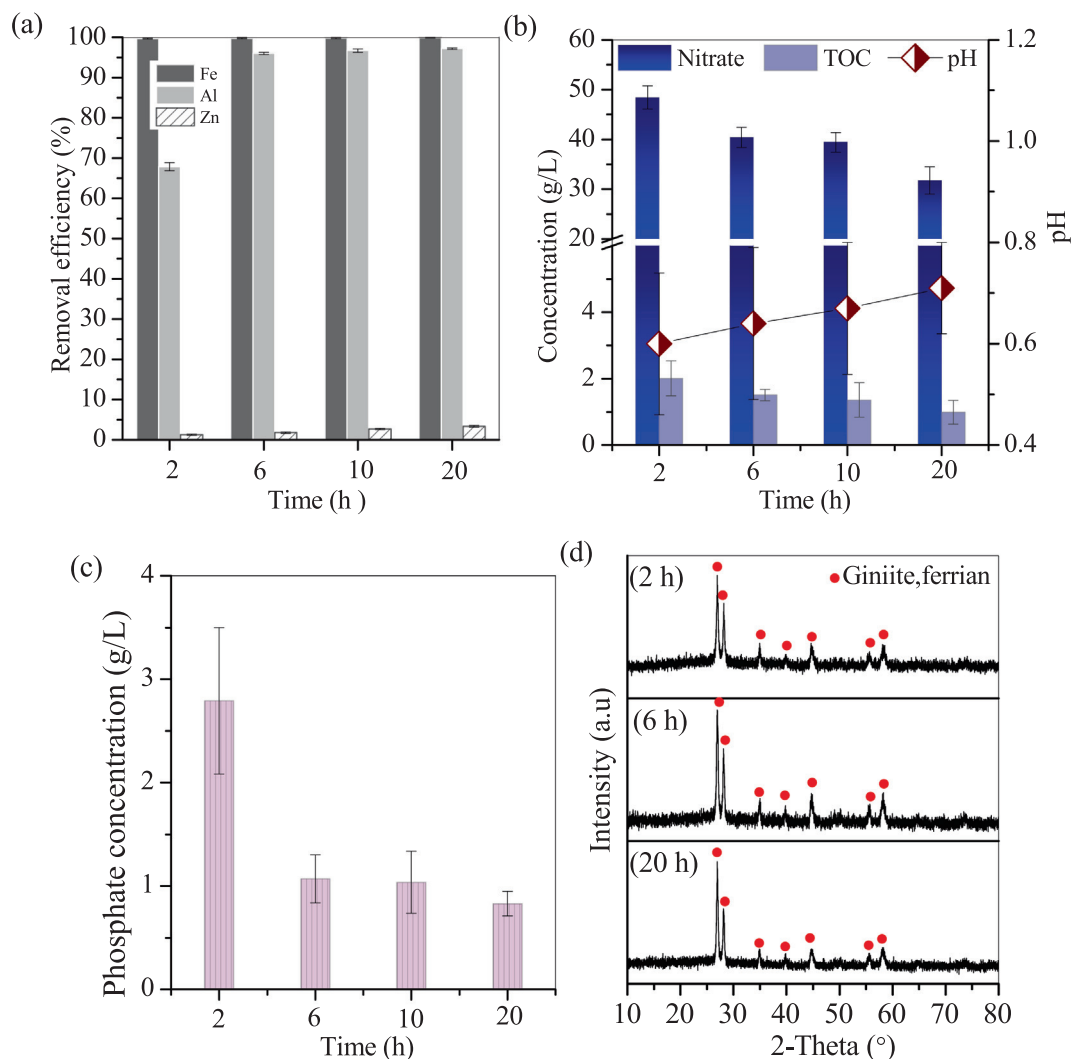


Fig. 9 (a) Removal efficiencies of Fe/Al/Zn; (b) Variation of solution pH, TOC, nitrate and (c) Variation of phosphate concentrations; and (d) XRD patterns of deposits generated at 2, 6 and 20 h.

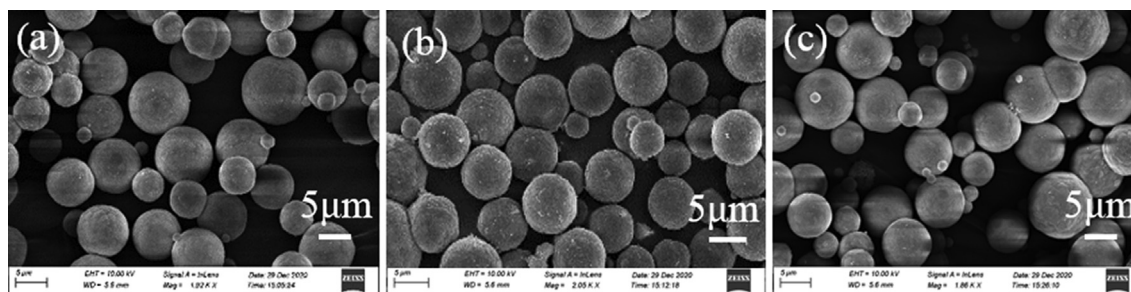


Fig. 10 SEM images of the deposits generated at 2, 6 and 20 h.

The hydrothermal precipitation of Al and phosphate was also performed without Fe to investigate the Al-bearing product in the presence of phosphate. The results showed only typical AlPO_4 peaks and irregular blocks (Fig. S1), indicating that the major product of Al and phosphate was AlPO_4 when Fe was absent in the solution. Given that pure AlPO_4 crystal

was not formed in Fe/Al-bearing solution, the removed Al was involved in the Fe precipitation of giniite sphere. Thus, a new route for the precipitation of Fe/Al with phosphate (Eqs. (3) and (5)) different from the formation of Fe/Al oxyhydroxide was proposed. Nearly 11 mol H^+ was released to generate 1 mol giniite. Such H^+ was involved in the redox reaction

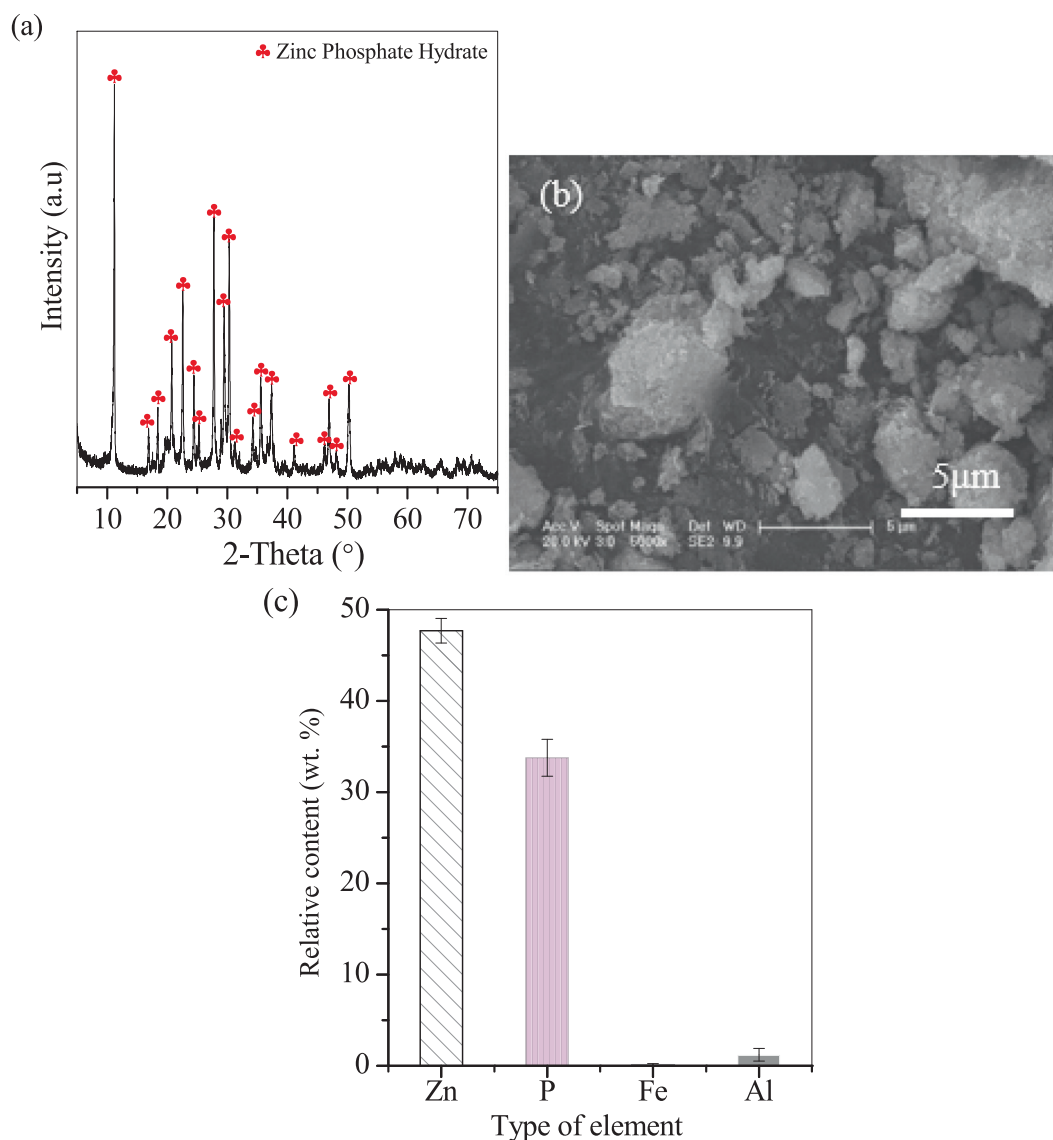
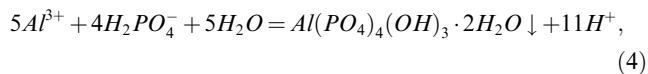
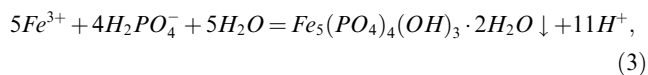
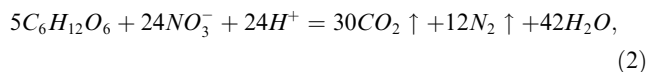
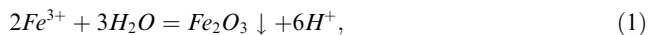


Fig. 11 (a) XRD pattern, (b) SEM image and (c) Major composition of Zn-bearing deposit.

of nitrate to glucose. When the solution pH increased correspondingly, giniite generation was promoted, resulting in the removal of Fe/Al at a high level.



After the reaction, the solution was at pH 0.6 and contained 0.14 g/L Al, where the corresponding Gibbs value for Al hydrolysis was -1.2 kJ/mol, which was close to zero. This find-

ing showed that the precipitation reaction of Al to phosphate was in equilibrium. When the solution pH was above 1, the precipitation of the remaining Al continued, but that of Zn also started (Figs. 7a and 12d), which was not desirable for Zn recovery.

3.5. Environmental applications

The proposed method showed its advantages in separating Fe/Al efficiently and recovering Zn as high-purity products. Other wastes, e.g. electronic waste (Olafsoye et al., 2013) and smelting residue (Gorai et al., 2003), also contained heavy metals and Fe/Al impurities and can be treated with this technique for recycling heavy metals. Other low-grade precious metal minerals, e.g. brookite, galena and millerite (Chen 2010), were also rich in Fe and Al that could be recovered using this method. Additionally, the recovered Fe/Al products were highly purified and have potential application in the production of electronic devices (Rueff et al., 2016), biological materials (Nedkov et al., 2016) and battery materials (Hong et al.,

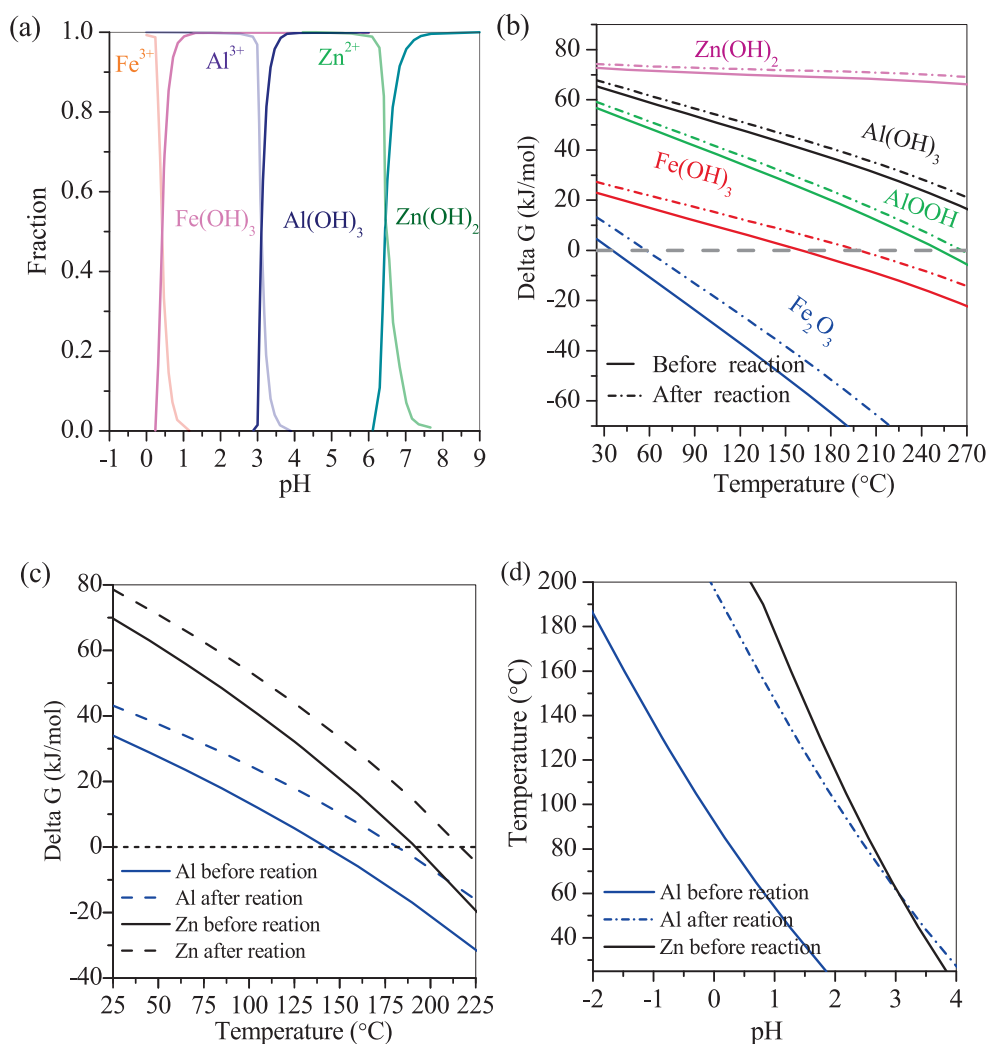


Fig. 12 (a) Hydrolysis diagram of Fe/Al/Zn at room temperature, (b) Gibbs free energies of Fe/Al/Zn hydrolysis with glucose and without phosphate (Before reaction: pH = 0.25, concentrations of Fe/Al/Zn were 10372, 3593 and 3093 mg/L, respectively; After reaction: pH = 0.82, concentrations of Fe/Al/Zn were 146.6, 3552.5 and 3045.4 mg/L, respectively) and (c) Gibbs free energies and (d) pH versus temperature of Fe/Al/Zn hydrolysis in the presence of phosphate (Before reaction: pH = 0.25, concentrations of Fe/Al/Zn were 10372, 3593 and 3093 mg/L, respectively, and concentration of phosphate was 15000 mg/L; After reaction: pH = 0.64, concentrations of Fe/Al/Zn were 20.7, 139 and 3038 mg/L, respectively, and concentration of phosphate was 1070 mg/L).

2003). However, this method also generated rest solution with abundant nitrate and phosphate. Future investigations should focus on the recovery of other valuable metals from Fe/Al-bearing hazardous waste and the recycling possibility of rest solution with high concentrations of nitrate and phosphate.

4. Conclusion

Cationic Zn was enriched from electroplating wastewater and recovered as valuable Zn phosphate hydrate with 98.1 wt% Zn₃(PO₄)₂·2H₂O. Such performance started with the coagulation of wastewater by commercial PAFC to produce Zn-rich sludge that was then leached by a mixed hydrochloric and nitric acid to form an acid solution comprising abundant Fe, Al and Zn. After hydrothermal treatment in the presence of phosphate and glucose, more than 99% and 96% Fe/Al were effectively precipitated as giniite sphere. Approximately 98% of Zn was kept in the remaining solution that can be neutralised to pre-

cipitate Zn as Zn phosphate hydrate. The proposed route showed practical application in the separation of impure Fe/Al from acid solution with high retention of heavy metals.

Declaration of Competing Interest

The authors declare that they have no known competing financial interests or personal relationships that could have appeared to influence the work reported in this paper.

Acknowledgments

This work was supported by the National Key Research and Development Program of China (Grant No. 2019YFE0117900), the National Natural Science Foundation of China (Grant Nos. 51878134 and 52070038) and the Science

and Technology Program of Jilin Province (Grant No. 20190303001SF) and the Innovative Research Team Program of Jilin Province (No. 20210509043RQ).

Appendix A. Supplementary material

Supplementary data to this article can be found online at <https://doi.org/10.1016/j.arabjc.2021.103664>.

References

- Amano, Y., Watanabe, K., Tashiro, S., Yamane, Y., Ishikawa, J., Yoshida, K., Uchiyama, G., Abe, H., 2015. Trends of nitrogen oxide release during thermal decomposition of nitrates in highly active liquid waste. *Trans. Atomic. Ener. Soc. Jpn.* 14, 86–94.
- Bahrodin, M.B., Zaidi, N.S., Hussein, N., Sillanp, M., Prasetyo, D.D., Syafiuddin, A., 2021. Recent advances on coagulation-based treatment of wastewater: transition from chemical to natural coagulant. *Curr. Pollut. Rep.* 138, 1–13.
- Bian, R., Su, T., Chen, Y., Qu, Z., Li, T., 2021. High-performance Al separation and Zn recovery from a simulated hazardous sludge. *Arab. J. Chem.* 14, 102996.
- Chen, X., 2010. Experimental study on processing technology of low grade molybdenum ore from inner mongolia. *Min. Metall. Eng.* 30, 40–43.
- China, M. o. E. a. E. o. t. P. s. R. o. Emission standard of pollutants for electroplating. GB 21900—2008.
- Dai, S., Wang, N., Qi, C., Wang, X., Wang, X., 2019. Preparation of core-shell structure $\text{Fe}_3\text{O}_4@\text{C}@\text{MnO}_2$ nanoparticles for efficient elimination of U(VI) and Eu(III) ions. *Sci. Total. Environ.*, p. 685.
- Daocheng, L., Lihui, Z., 2009. Study on the Treatment of waste water containing heavy metal ions by humic acid resin. *Henan. Chem. Ind.*
- Dessouky, S., El-Nadi, Y.A., Ahmed, I.M., Saad, E.A., Daoud, J.A., 2008. Solvent extraction separation of Zn(II), Fe(II), Fe(III) and Cd(II) using tributylphosphate and CYANEX 921 in kerosene from chloride medium. *Chem. Eng. Process.* 47, 177–183.
- Esm, A., Al, B., Rmm, A., Aea, C., 2020. Advanced eco-friendly and adsorptive membranes based on Sargassum dentifolium for heavy metals removal, recovery and reuse. *J. Water Process Eng.* 37, 101424.
- Fl, A., Shan, H.A., Chao, W.B., Mq, A., Lj, A., Bh, A., 2021. Adsorption and reduction of Cr(VI) from aqueous solution using cost-effective caffeic acid functionalized corn starch. *Chemosphere.*
- Gopala, A., Kipphardt, H., Matschat, R., Panne, U., 2010. Process methodology for the small scale production of m6N5 purity zinc using a resistance heated vacuum distillation system. *Mater. Chem. Phys.* 122, 151–155.
- Gorai, B., Jana, R.K., Premchand, 2003. Characteristics and utilisation of copper slag—a review. *Resour. Conservat. Recy.* 39, 299–313.
- Han, C., Zhoumin, Ye, Q., Yao, L., Xu, Z., 2016. Controllable synthesis of sphere and star-like $\text{Fe}_5(\text{PO}_4)_4(\text{OH})_3 \cdot 2\text{H}_2\text{O}$ microcrystals for effective photo-fenton-like degradation of rhodamine B. *Synth. React. Inorg. M.* 47.
- Hong, Y.S., Ryu, K.S., Chang, S.H., 2003. New iron-containing electrode materials for lithium secondary batteries. *Etri. J.* 25, 412–417.
- Hosseini, S.S., Bringas, E., Tan, N.R., Ortiz, I., Ghahramani, M., Shahmirzadi, M.A.A., 2016. Recent progress in development of high performance polymeric membranes and materials for metal plating wastewater treatment: a review. *J. Water. Pro. Eng.* 9, 78–110.
- Huajun, Z., Zhenghai, G., Yunpeng, Z., 2008. Electrorefining zinc dross in ammoniacal ammonium chloride system. *Hydrometallurgy* 90, 8–12.
- Huang, Y., Zhang, Z., Cao, Y., Han, G., Dou, Z., 2020. Overview of cobalt resources and comprehensive analysis of cobalt recovery from zinc plant purification residue – a review. *Hydrometallurgy* 193, 105327.
- Kim, C., Lee, B., Park, Y., Park, B., Lee, J., Kim, H., 2007. Iron-phosphate/platinum/carbon nanocomposites for enhanced electrocatalytic stability. *App. Phys. Lett.* 91, 345.
- Li, D., Zhang, B., Ou, X., Zhang, J., Xu, J., 2020. Ammonia leaching mechanism and kinetics of LiCoO₂ material from spent lithium-ion batteries. *Chin. Chem. Lett.* 32, 2333–2337.
- Li, J., Ma, H., 2017. Zinc and lead recovery from jarosite residues produced in zinc hydrometallurgy by vacuum reduction and distillation. *Green Process. Synth.*, 7
- Liu, C., Han, Q., Chen, Y., Zhu, S., Su, T., Qu, Z., Gao, Y., Li, T., Huo, Y., Huo, M., 2021a. Resource recycling of Mn-rich sludge: effective separation of impure Fe/Al and recovery of high-purity Hausmannite. *ACS Omega* 6, 7351–7359.
- Liu, F., Hua, S., Wang, C., Hu, B., 2021b. Insight into the performance and mechanism of persimmon tannin functionalized waste paper for U(VI) and Cr(VI) removal. *Chemosphere* 132199.
- Liyang, Z., Liang, Z., Jun, L., Yu, T., Baojun, L., 2004. Development of cold rolled and zinc coated steel sheet for auto special steel. *Spec. Steel-Huangshi* 25, 1–6.
- Mandal, B., Ghosh, S., Basumallick, I., 2010. Synthesis of mesoporous FePO_4 cathode material for its application in rechargeable lithium-ion batteries. *Electrochem. Soc.*
- Martins, P.M., Salazar, H., Aoudjit, L., Goncalves, R., Lanceros-Mendez, S., 2021. Crystal morphology control of synthetic giniite for enhanced photo-Fenton activity against the emerging pollutant metronidazole. *Chemosphere* 262, 128300.
- Meng, L., Zhong, Y., Guo, L., Wang, Z., Chen, K., Guo, Z., 2018. Recovery of Cu and Zn from waste printed circuit boards using super-gravity separation. *Waste Manage.* 78, 559–565.
- Ming, M., He, D., Liao, S., Yue, Z., Yao, S., 2002. Kinetic study of l-isoleucine transport through a liquid membrane containing di(2-ethylhexyl) phosphoric acid in kerosene. *Anal. Chim. Acta* 456, 157–165.
- Muneyama, E., Kunishige, A., Ohdan, K., Ai, M., 1996. Reduction and reoxidation of iron phosphate and its catalytic activity for oxidative dehydrogenation of isobutyric acid. *J. Catal.* 158, 378–384.
- Nedkov, I., Groudeva, V., Angelova, R., Iliev, M., Liu, C., Wang, X., Qu, Z., Zhang, Y., Zhang, H., 2016. New iron oxides/hydroxides biomaterials for application in electronics and medicine. *Mach. Technol. Mater.* 10, 48–51.
- Newbury, D., Ritchie, N., Bright, D., 2009. Characterizing heterogeneous particles with SEM/SDD-EDS mapping and NIST Lispix. *Proc. Spie. Int. Soc. Opt. Eng.*, 7378
- Nogueira, C.A., Margarido, F., 2015. Selective process of zinc extraction from spent Zn–MnO₂ batteries by ammonium chloride leaching. *Hydrometallurgy* 157, 13–21.
- Olafisoye, O.B., Adefioye, T., Osibote, O.A., 2013. Heavy metals contamination of water, soil, and plants around an electronic waste dumpsite. *Pol. J. Environ. Stud.*
- Park, S.M., Yoo, J.C., Ji, S.W., Yang, J.S., Baek, K., 2014. Selective recovery of dissolved Fe, Al, Cu, and Zn in acid mine drainage based on modeling to predict precipitation pH. *Environ. Sci. Pollut. R.* 22, 3013–3022.
- Harrison, P.G., Begley, M.J., Kikabhai, T., Killer, F., 1986. Zinc(II) bis(O, O'-dialkyl dithiophosphates): complexation behaviour with pyridine and other multidentate nitrogen donor molecules. The crystal and molecular structures of the 1:1 complexes of bis(O, O'-di-isopropyl dithiophosphato)zinc(II) with pyridine. *J. Chem. Soc.*
- Pourjavid, M.R., Sehat, A.A., Hosseini, M.H., Rezaee, M., Jamali, M. R., 2014. Use of 2-(tert-butoxy)-N-(3-carbamothioylphenyl)acetamide and graphene oxide for separation and preconcentration of Fe(III), Ni(II), Cu(II) and Zn(II) ions in different samples. *Chin. Chem. Lett.* 25, 791–793.

- Qu, Z., Su, T., Chen, Y., Lin, X., Yu, Y., Zhu, S., Xie, X., Huo, M., 2019. Effective enrichment of Zn from smelting wastewater via an integrated Fe coagulation and hematite precipitation method. *Front. Environ. Sci. En.* 13, 94.
- Qu, Z., Su, T., Zhu, S., Chen, Y., Bian, D., 2021. Stepwise extraction of Fe, Al, Ca, and Zn: a green route to recycle raw electroplating sludge. *J. Environ. Manage.* 300, 113700.
- Rahman, M.L., Zhi, J.W., Sarjadi, M.S., Abdullah, M.H., Heffernan, M.A., Sarkar, M.S., O'Reilly, E., 2021. Poly(hydroxamic acid) ligand from palm-based waste materials for removal of heavy metals from electroplating wastewater. *J. Appl. Polym. Sci.*, 138
- Rossini, G., Bernardes, A.M., 2006. Galvanic sludge metals recovery by pyrometallurgical and hydrometallurgical treatment. *J. Hazard. Mater.* 131, 210–216.
- Rueff, J.M., Poienar, M., Guesdon, A., Martin, C., Maignan, A., Jaffres, P.A., 2016. Hydrothermal synthesis for new multifunctional materials: a few examples of phosphates and phosphonate-based hybrid materials. *J. Solid. State. Chem.*
- Rueff, J.-M., Poienar, M., Guesdon, A., Martin, C., Maignan, A., Jaffrès, P.-A., 2016. Hydrothermal synthesis for new multifunctional materials: a few examples of phosphates and phosphonate-based hybrid materials. *J. Solid State Chem.* 236, 236–245.
- Sadeghi, S.M., Vanpeteghem, G., Neto, I., Soares, H., 2017. Selective leaching of Zn from spent alkaline batteries using environmentally friendly approaches. *Waste Manage.* 60, 696.
- Samaniego, H., Román, M.S., Ortiz, I., 2006. Modelling of the extraction and back-extraction equilibria of zinc from spent pickling solutions. *Sep. Sci. Technol.* 41, 757–769.
- Song, S., Sun, W., Wang, L., Liu, R., Han, H., Hu, Y., Yang, Y., 2019. Recovery of cobalt and zinc from the leaching solution of zinc smelting slag. *J. Environ. Chem. Eng.*, 7
- Su, T., Bian, R., Chen, Y., Zhu, S., Huo, Y., Liu, J., 2020a. Improvement of a hydrometallurgical process for recovering Mn from electric-arc furnace slag. *Miner. Eng.* 159, 106644.
- Su, T., Han, Z., Qu, Z., Chen, Y., Xie, X., 2020b. Effective recycling of Co and Sr from Co/Sr-bearing wastewater via an integrated Fe coagulation and hematite precipitation approach. *Environ. Res.* 187, 109654.
- Wahaab, R.A., Moawad, A.K., Taleb, E.A., Ibrahim, H.S., El-Nazer, H., 2013. Combined photocatalytic oxidation and chemical coagulation for cyanide and heavy metals removal from electroplating wastewater. *World. Appl. Sci. J.*, 19
- Wang, B., Li, Y., Zheng, J., Hu, Y., Hu, B., 2020. Efficient removal of U(VI) from aqueous solutions using the magnetic biochar derived from the biomass of a bloom-forming cyanobacterium (*Microcystis aeruginosa*). *Chemosphere* 254, 126898.
- Wang, L.P., Chen, Y.J., 2019. Sequential precipitation of iron, copper, and zinc from wastewater for metal recovery. *J. Environ. Eng.*, 145
- Weert, G.V., Sandwijk, T.V., Hogeweg, P., 1998. Solvent extraction of ferric iron from zinc sulphate solutions with DEHPA – investigation of nitric acid as stripping agent.
- Yang, S., Li, Q., Chen, L., Chen, Z., Wang, X., 2019. Ultrahigh sorption and reduction of Cr(VI) by two novel core-shell composites combined with Fe₃O₄ and MoS₂. *J. Hazard. Mater.* 379, 120797.
- Yu, L., Han, M., He, F., 2017. A review of treating oily wastewater. *Arab. J. Chem.*, 10
- Yw, A., Ji, A., Yan, G.B., Yang, Y.A., Yang, G.A., Zx, A., 2019. Removal of aluminum from rare-earth leaching solutions via a complexation-precipitation process. *Hydrometallurgy* 191.
- Zhao, J., Huang, R.M., Nie, L.Y., Luo, Q., 2010. Study on treatment of copper and nickel electroplating wastewater by Fenton oxidation–biological aerated filter process. *Electrop. Finish.* 29, 36–38.
- Zhong, X., Lu, Z., Liang, W., Hu, B., 2020. The magnetic covalent organic framework as a platform for high-performance extraction of Cr(VI) and bisphenol a from aqueous solution – ScienceDirect. *J. Hazard Mater.*, 393
- Zhong, X.H., Jiao, F., Qin, W.Q., Wang, D.W., 2017. Review on treatment and disposal methods of electroplating sludge. *Electrop. Finish.* 36, 948–953.
- Zhu, S., Wang, Z., Lin, X., Sun, T., Huo, Y., 2020. Effective recycling of Cu from electroplating wastewater effluent via the combined Fenton oxidation and hydrometallurgy route. *J. Environ. Manage.* 271, 110963.